





Article

The Creation of a Multiallele Knockout Genotype in Rabbit Using CRISPR/Cas9 and Its Application in Translational Medicine

Tímea Pintér^{1,2}, Miklós Geiszt³, Gábor L. Petheő³ , Máté Mihálffy³, Gabriella Skoda¹, Nándor Lipták¹ , Andrea Kerekes¹, Zsuzsanna Bősze¹, László Hiripi^{1,2,*}  and Lilla Bodrogi^{1,*} 

¹ Rabbit Genome Biology and Biodel Group, Department of Animal Biotechnology, National Agricultural Research and Innovation Center, Szent-Györgyi Albert str. 4, 2100 Gödöllő, Hungary; pinter.timea@abc.naik.hu (T.P.); skoda.gabriella@abc.naik.hu (G.S.); liptak.nandor@abc.naik.hu (N.L.); kerekes.andrea@abc.naik.hu (A.K.); bosze.zsuzsanna@abc.naik.hu (Z.B.)

² Institute of Genetics and Biotechnology, Szent István University, Páter Károly str. 1, 2100 Gödöllő, Hungary

³ Department of Physiology, Faculty of Medicine, Semmelweis University, Üllői str. 26, 1085 Budapest, Hungary; geiszt.miklos@med.semmelweis-univ.hu (M.G.); petheo.gabor@med.semmelweis-univ.hu (G.L.P.); mihalfy.mate@med.semmelweis-univ.hu (M.M.)

* Correspondence: hiripi1@gmail.com (L.H.); bodrogi1@gmail.com (L.B.)

Received: 29 October 2020; Accepted: 25 November 2020; Published: 28 November 2020



Abstract: Nonrodent animal models have recently become more valuable in preclinical studies. The limitation of nonrodent animal models is that they must demonstrate relatively reliable and predictable responses in addition to representing complex etiologies of a genetically diverse patient population. In our study, we applied CRISPR/Cas9 technology to produce transgenic rabbits. This approach can be useful for creating genetically divergent and homogeneous populations for studies in translational medicine. NADPH oxidase 4 (NOX4) is a promising therapeutic target, as it is linked to several pathologies including stroke, atherosclerosis, and lung and kidney fibrosis. NOX4 knockout (KO) rabbit lines were created in order to study the *in vivo* effects resulting from a lack of NOX4 protein and loss of gene function. One of the knockout founders was a germline multiallelic knockout male. Its offspring segregated into three distinct NOX4 knockout and a wild-type lines. Mosaicism is a relatively frequent phenomenon in rabbit transgenesis. Our results point to the possible application of mosaicism in preclinical studies. However, careful planning and evaluation of results are necessary. The predicted off-target sites were studied as well, and no signs of off-target events were detected.

Keywords: NADPH oxidase 4; NOX4; CRISPR/Cas9; transgenic rabbit; rabbit gene knockout; germline multiallelic knockout; mosaicism; translational medicine

1. Introduction

Since the creation of the first genetic knockout rabbits with the CRISPR/Cas9 method in 2014 [1], the number of publications on CRISPR/Cas9-modified rabbits has increased, touching on a wide array of topics such as improving meat quality [2], altering fur color [3], studying the metabolic features [4,5], modeling human diseases [6], producing recombinant proteins [7], and improving the methodology [8–10]. Compared to rodents, rabbits are phylogenetically more closely related to humans, and many physiological processes, such as lipid and carbohydrate metabolism [11,12], disease progression in the case of atherosclerosis [13,14], cardiac diseases [15], and obesity [16,17], are more similar to those in humans. In addition, because of their similar anatomy and bigger size,

experimentation is more achievable with rabbits, and they are hence considered to be a better subject for studies in translational medicine [18].

CRISPR/Cas9 technology in animal transgenesis has undergone great improvements in recent years. Prior to the employment of this technique, it was a big challenge to knockout a gene in rabbits because of the lack of suitable embryonic stem cells [19–21] and the low efficiency and difficulties associated with rabbit somatic cell nuclear transfer [22]. Now, with the almost completely sequenced rabbit genome and expertise available, CRISPR/Cas9 is a relatively robust technology that can be used to knockout almost any gene in rabbits. Knocking out a gene with CRISPR/Cas9 is based on targeted cutting of double-stranded DNA and the cells' own mechanism of DNA damage repair by nonhomologous end joining (NHEJ), resulting in indels at the target site that usually result an early stop codon that leads to fast degradation of mRNA [23,24].

In order to reduce the number of experimental animals and test mutations rapidly, embryo culturing and testing for mutations at the blastocyst stage are suitable alternatives. In mice, in vitro cultured preimplantation stage blastocysts have been appropriate for testing the fidelity of CRISPR/Cas9-mediated genome editing [25].

Concerns remain about the unwanted off-target effects of CRISPR/Cas9 technology. However, modified Cas9 enzymes with higher specificity and improved algorithms that allow researchers to choose the most suitable guide RNA (gRNA) provide a stable background to overcome this challenge [26,27].

Genetic mosaicism of founder animals is a known phenomenon in CRISPR/Cas9-mediated gene editing, as summarized in the review of Mehravar et al. [28]. CRISPR/Cas9 is directly injected into the cytoplasm or pronuclei of fertilized oocytes. As zygotes develop, cells continuously divide, and the CRISPR-directed Cas9 enzyme is able to cut the targeted locus at further stages of development. As a consequence, somatic and/or germline mosaicism develops in the founder animals [28]. Mosaicism was investigated in mice, for example, as described by the authors of [29,30], following the injection of CRISPR/Cas9 components targeting the tyrosinase gene locus, revealing the occurrence of diverse allelic modifications of the tyrosinase gene and also affecting the germline of the founder animals. However, in most cases, the germline cells of the founder animal carry only one type of modified allele. Interestingly, mosaicism in founder transgenic rabbits appears more frequently than in mice. Early rabbit embryos undergo a rapid series of cell divisions and can reach the four-cell stage within half a day [31]. In humans, rodents, and livestock animals, this takes 30–40 h after fertilization. The early timing of differentiation can explain the high mosaicism rates during rabbit transgenesis [32]. Despite the high rate of mosaicism in transgenic rabbits, to our best knowledge, a germline multiallelic knockout rabbit has not previously been described.

NADPH oxidase 4 (NOX4) is an important and widely expressed member of the NADPH oxidase family that is responsible for the production of reactive oxygen species (ROS). NOX4 is an important regulatory protein for many cellular processes, including cell division and differentiation [33], apoptosis [34], host defense [35], and oxygen sensing [36], in addition to contributing to gene regulatory pathways [37,38]. In mammals, including rabbits, humans, and rodents, its main expression site is the kidney [39], and it is also expressed in many other tissues, such as lung, liver, and brain. NOX4 plays an important role in many pathologies, including in stroke [40] and lung [41] and kidney fibrosis [42]. It also regulates the development of atherosclerosis [43,44]. The rabbit is a classical model animal in atherosclerosis research [13,14,45], making rabbit knockouts an ideal subject to study the lack of NOX4 gene function in the course of atherosclerosis.

Animal models in translational medicine usually share similar molecular targets, pathways, or phenotypes with humans. They can be very useful for predicting human responses, although ethical controversies regarding the use of experimental animals have arisen in the last century [46]. Besides rodents, most preclinical animal studies typically require one additional nonrodent species [47]. The use of nonrodents would increase the sensitivity of different tests for human applications [48]. An important disadvantage of nonrodent models is their genetic diversity, which can lead to differences

in physiology and metabolism, as in the case of dog models [49]. Thus, inbred animals (and even nuclear-cloned animals) are the most controlled model systems, and their use can bypass several challenges associated with human studies [50]. On the other hand, biology is characterized by diversity as well as unity [51]. To avoid the questionable validity of an animal model system, genetic diversity should be assured. The dual problem of genetic diversity in animal model systems can be solved using mosaicism in transgenic founders of nonrodent species. In this paper, we show that a transgenic rabbit founder animal can produce multiallelic germline knockout strains that can be maintained as a closely related animal population and with high genetic diversity. Both are necessary for successful translational medical studies.

2. Materials and Methods

2.1. Ethics Statement

The rabbits used in this study were New Zealand white rabbits (Innovo Ltd., Isaszeg, Hungary). All animal studies were conducted in strict accordance with the recommendations and rules in the Hungarian Code of Practice for the Care and Use of Animals for Scientific Purposes, approved by the Animal Welfare and Research Ethics Committee at Agricultural Biotechnology Institute, National Agricultural Research and Innovation Centre (NARIC-ABC) and registered under permission number ÁK-ENG (PE/EA/58-2-2018) from Pest County's governmental office. All efforts were made to minimize the suffering of animals.

2.2. Animals

Laboratory rabbits were maintained in the Animal Care Facility at NARIC-ABC. Animals were housed in individual cages with free access to food and water. Animals were kept under a standard light–dark cycle (06.00–18.00 h) at 19 °C.

2.3. Microinjection and Embryo Transfer

The protocol for superovulation of embryo donor does, embryo collection, microinjection of pronuclear-stage embryos, and transfer to recipient females has been described in our previous paper [52].

In summary, sexually mature does received an intramuscular injection of pregnant mare serum gonadotropin (PMSG) (ProSpec, Rehovot Israel), followed by an intravenous injection of human chorionic gonadotropin (hCG) (Choragon, Ferring GmbH, Kiel, Germany) 72 h later in order to induce superovulation. Donor rabbits were mated after the hCG injection. The oviducts were flushed with PBS–20%FCS (vol/vol) medium for collection of pronuclear-stage embryos. Zygotes were incubated in a Nuaire thermostat (38.5 °C, 5% CO₂, 80% humidity) in the same embryo culture medium. A mixture of synthetic gRNA and transactivating RNA (Sigma-Merck, Budapest, Hungary) was added to capped Cas9 RNA (150 ng/μL) (Trilink, San Diego, CA, USA) to a final concentration of 5 ng/μL in an embryo microinjection buffer (1 mM Tris, pH 7.5, 0.1 mM EDTA). Cas9 mRNA is a highly purified capped form by CleanCap® technology preventing 5' degradation and with increased half-life of mRNA. An aliquot of each batch used for microinjection was checked for degradation. Each batch was kept at 37 °C for 4 h previous to microinjection followed by agarose electrophoresis. Without any visible sign of degradation, RNA solution was ready for microinjection and the solution was injected into the cytoplasm of pronuclear-stage embryos. The injected embryos were incubated in embryo culture medium for 2–3 h, followed by the transfer of approximately 30–40 injected embryos into the oviducts of each recipient mother via laparoscopic surgery [52].

Guide RNA was designed using the publicly available E-CRISP program (<http://www.e-crisp.org/E-CRISP/designcrispr.html>) according to the second and fourth exon of the *NOX4* gene (chromosome 1: 127,338,844–127,541,489, ENSOCUG00000016685.4). Guide RNAs are shown in Figure 1.

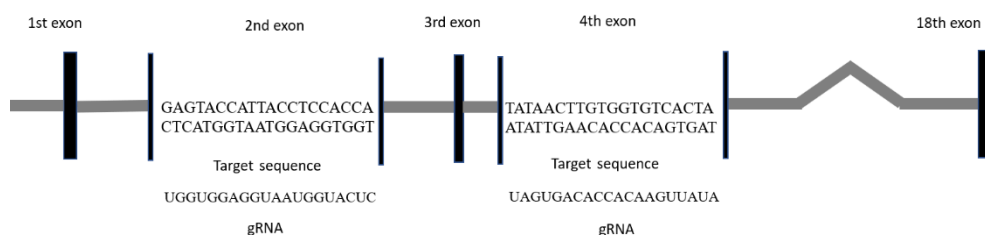


Figure 1. These guide RNAs targeting the second and fourth exons of the rabbit NADPH oxidase 4 gene for the CRISPR/Cas9 system. The second exon gRNA with PAM sequence is UGGUGGAGGUA AUGGUACUC-TGG. The fourth exon gRNA with PAM sequence is UAGAGCACCACAAGUUUAUA-TGG.

2.4. DNA Isolation from Blastocysts and Newborn Pups

Injected zygotes were individually collected at the blastocyst stage with a minimal amount of culture media in a 200 μ L standard PCR microtube (Merck, Budapest, Hungary) and air-dried. Then, 5 μ L of water was added and incubated at 95 $^{\circ}$ C for 5 min, followed by a 10 min incubation at -70° C. This process was repeated twice. Embryos were then incubated in a 200 μ L final volume of lysis buffer (10 mM Tris pH 8.0, 100 mM NaCl, 10 mM EDTA pH 8.0, 0.5% SDS, 0.4 mg/mL proteinase K) at 37 $^{\circ}$ C for 2 h. DNA was isolated using the phenol-chloroform method. Equal volumes of phenol and chloroform were added to the mixture, shaken thoroughly, and centrifuged at 13,000 rpm for 10 min. The supernatant was mixed with a double volume of isopropanol, kept at -70° C overnight, and centrifuged for 30 min at 4 $^{\circ}$ C. The resulting invisible pellet was then washed twice with 70% ethanol, air-dried, and dissolved in 10 μ L water. Genomic DNA from tissue samples was isolated using the conventional phenol-chloroform method [53].

2.5. Detection of Mutations in Embryos and Pups by PCR and Sequencing

The PCR primers used for mutation detection and Sanger sequencing are listed in Table 1. PCR reactions were set up with RedTaq Ready mix (Sigma, Budapest, Hungary) with standard PCR conditions (96 $^{\circ}$ C for 5 min; 33 cycles of 95 $^{\circ}$ C for 15 s, 58 $^{\circ}$ C for 15 s, 72 $^{\circ}$ C for 20 s; and a final step of 72 $^{\circ}$ C for 5 min followed by holding at 4 $^{\circ}$ C) in a ProFlex PCR system thermal cycler (Applied Biosystems, Budapest, Hungary).

Table 1. PCR primers used for mutation detection and sequencing.

Primer	Sequence	Product Size (Base Pairs)
2. exon-forward	TTGCTTGGATTTACCCCTGC	312
2. exon-reverse	AGTCTGGTGGCTAAGTCTGC	
4. exon-forward	ACATCTCACCAACGTTTGA	386
4. exon-reverse	TAGACAATCATATTTAAAC	
2nd exon seq. primer-forward	CAACTAACAAACTTGACGCC	1059
2nd exon seq. primer-reverse	AAGCCACTGAAAAACACCC	

PCR products were gel purified with NucleoSpin Gel and PCR Clean up Columns for gel extraction and a PCR cleanup kit (Macherey Nagel, Dueren, Germany) and cloned into pGEM-T vector (pGEM-T Easy Vector System I, Bioscience, Budapest, Hungary). Then, 4–5 PCR-positive plasmid clones were sequenced. Chromas software (Technelysium Pty Ltd., South Brisbane, Australia) was used for sequence analysis.

2.6. T7 Endonuclease I Assay

A T7 endonuclease I assay was performed to detect mutations in the target sequence [54]. After the extraction of genomic DNA from blastocysts and pups, the genomic region of *NOX4* was PCR amplified

(primers are shown in Table 1). The PCR product was denatured and reannealed under the following conditions: 95 °C for 5 min, 95–85 °C at –2 °C/s, 85–25 °C at –0.1 °C/s, holding at 4 °C. The reannealed fragments were digested with T7EI (NEB, Ipswich, MA, USA), separated, and visualized on an ethidium bromide-stained 2% agarose gel.

2.7. Off-Target Assay

Potential off-target sites of the sgRNAs were predicted using the CRISPR online design tool CRISPR/Cas-OFFinder RGEN (<http://www.rgenome.net/cas-offinder/>). The eight most promising off-target sites for *NOX4* second exon sgRNAs were chosen for PCR and sequencing using REDTaq[®] ReadyMix (Sigma Aldrich, Budapest, Hungary) with the corresponding primers (Table 2). PCR products were analyzed on a 2% agarose gel, then purified and directly Sanger sequenced (Eurofins Genomics, Ebersberg, Germany). Chromas software and online blast tool (https://www.ensembl.org/Oryctolagus_cuniculus/Tools/Blast) was used for sequence analysis and evaluation of results.

Table 2. The eight most potent off-target sites in the rabbit genome predicted by the CRISPR/Cas-OFFinder RGEN tool. Lowercase letters indicate the sites of mismatches compared to the target sequence.

Off-Targets	Off-Target Sequence Compared to Target DNA	Chromosome	Location	Number of Mismatches	Primers
<i>NOX4</i> 2nd exon target site	TGGTGGAGGTAATGGTACTCNGG	chr1	127339745	0	
Off-target-1	TGtGGtGGTAATGGTACTtGGG	chr1	135497670	3	forward AAGAGACAGGAGACAGGAAG reverse ATTAGGAAAGCAATGTGAGGG
Off-target-2	TGGTGGAGGTAATGGTgaTCGGG	chr10	31875932	2	forward AAAGACAACCGAAAGGCAG reverse AGCATAATGAGATTAAGCCCAG
Off-target-3	TGGaGGAGGTAATGaTcCTCTGG	chr11	37138594	3	forward ATGATGAGATGGAGGCAAGG reverse TGTGTGATTATTGGCCGAGA
Off-target-4	TGGTGGAGGTgATGGTgCTCAGG	chr14	81541288	2	forward TGACCCTTAACAGTCCCTCC reverse CCTAAACCCTACACCTACC
Off-target-5	TGaTGGAGGTAATGGTAItGGG	chr15	45312042	3	forward AGGAAGAAAGTAGGCCAGT reverse CTGCCAGCTGAGTTGTAGT
Off-target-6	TGGTGGtGGTggTGGTACTCTGG	chr2	99798645	3	forward GGGTGAACCAGCAGTAAAG reverse GTTCAGATAGACAGCCCCAG
Off target-7	TGGTGGAGaTAATGGgAtTCTGG	chr8	79971373	3	forward AAGAAACGTGCCAGGGGATT reverse TTAACCCTACGTCATGCC
Off target-8	TGGTgTAGGgAATGGTACTCCGG	chr9	111235794	2	forward GGTGTAATCCAGGAACAATGCT reverse CATGCCCCAGGACTGTAGAG

3. Results

3.1. Testing of Guides and Production of Founder Knockout Animals

The mutation efficiency of guide RNAs was tested in cultured blastocysts. Both guides were effective in inducing mutations in the rabbit *NOX4* gene. However, the guide RNA targeting the second exon of *NOX4* had slightly higher mutation efficiency. Table 3 shows the ratio of total injected zygotes that developed to blastocyst stage to mutant blastocysts for the two guides designed for the second and fourth exons (18% and 16%, respectively).

Table 3. Results of microinjection of Cas9 and targeting gRNAs into rabbit zygotes. The second and fourth exons were targeted, and both guides were successful in inducing targeting events with almost equal efficiency.

Targeted Exon of <i>NOX4</i>	Total/Mutant Blastocysts	Ratio
2nd exon	11/2	18%
4th exon	18/3	16%

In addition, it is beneficial to introduce an early stop codon in the second exon in order to avoid the presence of a functional truncated peptide. Hence, we chose the RNA guide targeting the second exon of the *NOX4* gene to produce live animals.

Based on the results of embryo testing, a total of five knockout founder animals were produced, two males and three females, as summarized in Table 4. All mutations were heterozygous 7 bp and 8 bp deletions directly upstream of the PAM site with a couple of base differences: Animals #2, #3 and #4 acquired identical mutations (Figure 2), while animal #5 carried three different mutated alleles. We established heterozygous and homozygous genome-edited rabbit sublines by consecutive brother–sister mating from founder animal #5.

Table 4. Summary of mutations in *NOX4* KO founder rabbits. One male (#1) and three female (#2–4) rabbits had 7–8 bp deletions. Male #5 carried three distinct alleles with alternative mutations.

Code of Founder Animal	Sex	Mutation	Consequence
#1	♂	7 bp deletion (GGTACTC)	early stop codon
#2	♀	8 bp deletion (TGGTACTC)	early stop codon
#3	♀	8 bp deletion (TGGTACTC)	early stop codon
#4	♀	8 bp deletion (TGGTACTC)	early stop codon
#5	♂	allele A: 8 bp deletion (ACTCTGGC) allele B: 128 bp deletion allele C: 104 bp deletion in total	early stop codon early stop codon early stop codon

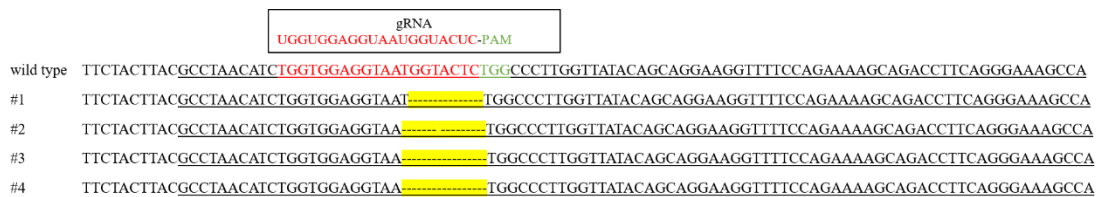


Figure 2. Comparison of mutations in *NOX4* knockout rabbit founders. The gRNA and the target in the gene followed by the PAM sequence are highlighted in red. The yellow spaces indicate the sites of mutation. The second exon is underlined with a black line. Animal #1 had a 7 bp deletion; #2–4 had identical 8 bp deletions. All four deletions were directly followed by the PAM sequence.

Animal #5 passed on four different alleles to the F1 generation (Figures 3 and 4). The most frequent allele was an 8 bp deletion ($\Delta 8$). The other allele contained a 128 bp deletion ($\Delta 128$), including an intronic region. The third allele type was the most irregular, with deletions and insertions adding up to a 104 bp deletion in total ($\Delta 104$) upstream of the PAM sequence. A wild-type allele also appeared in the F1 generation, demonstrating the presence of a fourth allele. We analyzed the expression level of *NOX4* in different tissues of a selected homozygous individual from line $\Delta 8$ by RT-qPCR. Expression pattern matched to an expected -/- phenotype (data not shown).

```

                                gRNA
                                UGGUGGAGGUAUUGGUACUC-PAM
wild type GGTAACCCAAGTTC TACTTACGCCTAACATCTGGTGGAGGTAATGGTACTCTGGCCCTTGGTTATACAGCAGGAAGGTTTTCCAGAAAAGCAGACCAITTCAG
Δ128 GGTAACCCAAGTTC TACTTACGCCTAACATCTGGTGGAGGT
Δ104 GGTAACCCAAGTTC TACTTACGCCTAACATCTGGTGGAGGTAA TGGCCCTTGGTTATACAGCANGAAGGTTTTCCAGAA AAGCA ACCAITCA
Δ8 GGTAACCCAAGTTC TACTTACGCCTAACATCTGGTGGGGTAATGGT CCTTGGTTATACAGCAGGAAGGTTTTCCAGAAAAGCAGACCAITTCAG

wild type GGAAAGCCAGATGAGCTAAACCAATCAAAGGGAGAGAGAAAAAATAAAAATAAACATTACCTATGAATGAAGACCACAAGTGTATTCTTAGAGAACTTT
Δ128 ATGAAGACCACAAGTGTATTCTTAGAGAACTTT
Δ104 GGAAAGCCAGATGTAAT
Δ8 GGAAAGCCAGATGAGCTAAACCAATCAAAGGGAGAGAGAAAAAATAAAAATAAACATTACCTATGAATGAAGACCACAAGTGTATTCTTAGAGAACTTT

wild type AAATGGGGCCTCAACTAGTAATTACAGAAAACATATGCAATGG
Δ128 AAATGGGGCCTCAACTAGTAATTACAGAAAACATATGCAATGG
Δ104 TAGTAATTACA AAAACATATGCAATGG
Δ8 AAATGGGGCCTCAACTAGTAATTACAGAAAACATATGCAATGG
    
```

Figure 3. Comparison of mutations originating from the #5 founder male. The gRNA and the target in the gene followed by the PAM sequence are highlighted in red. The yellow spaces show the sites of deletions. The second exon is underlined with a black line. The Δ8 mutation is a small deletion of eight base pairs, indicated in yellow. In Δ104, a TAAT insertion is present, highlighted in blue, and a couple of single base pair changes appeared in the sequence of Δ104 and Δ8, which, in the case of the Δ104 mutated allele, was probably the consequence of imperfect NHEJ repair. However, in the Δ8 mutated allele, it might be a small nucleotide polymorphism not related to NHEJ.

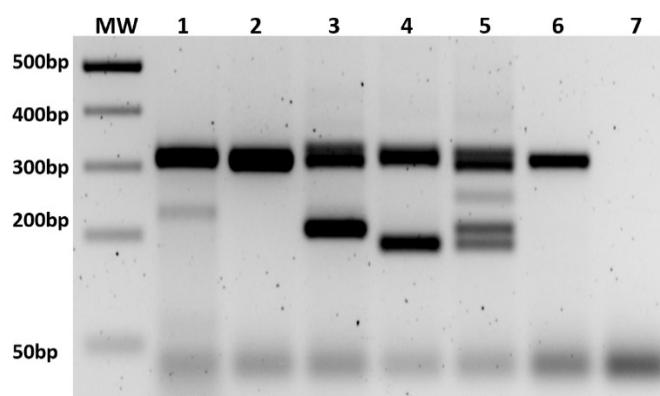


Figure 4. Detection of mutation is performed with PCR and/or T7 digestion. MW = molecular weight marker. (1–2) T7 assay and PCR of F1 heterozygous offspring of Δ8 line, respectively; (3–4) PCR of heterozygous offspring of Δ104 and Δ128 line, respectively; (5) PCR of founder male #5; (6–7) PCR of wild-type animal and no template control.

3.2. Off-Target Analysis

The selected potential off-target sites were amplified by PCR using genomic DNA from both the wild-type animal and founder rabbit #5 and evaluated by DNA sequencing. Eight candidate off-target sites were analyzed. In all these cases, no difference was observed (see Figure 5), so no off-target event was detected at any of the genomic locations.

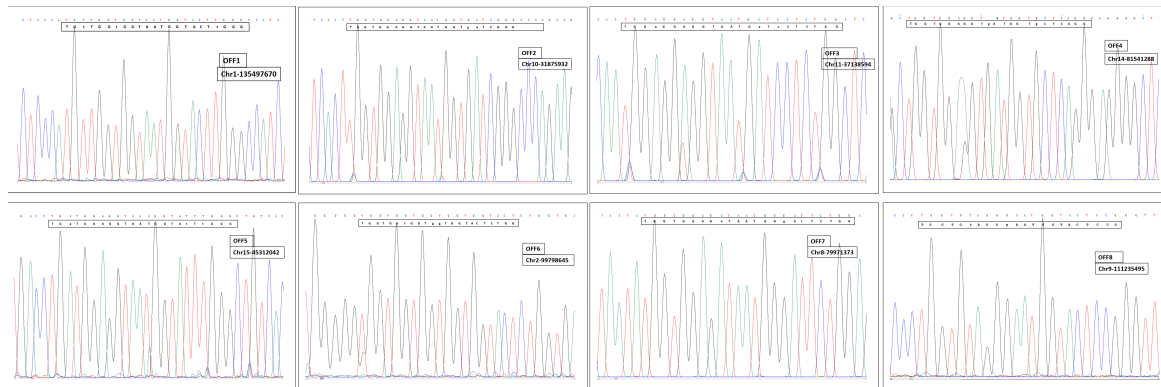


Figure 5. Sequence analysis of the eight candidate off-target sites predicted for *NOX4* second exon sgRNA.

3.3. Heritability of Deletions

Founder animal #5 was used as a sperm donor in four different artificial inseminations. Female partner animals originated from two different available sub-breeds of New Zealand White rabbits to represent different genotypes. Later, the same females were used in two more consecutive matings to represent animal populations with close relationships (both parents were the same). Animal #5, the founder male, had a total of four litters with an average litter size of 3–10 pups/litter. The three mutants and the wild-type allele appeared with varying frequencies among the pups in the F1 generation. The most frequent allele was $\Delta 8$ with 50%, followed by $\Delta 128$ and $\Delta 104$ with 36% and 10%, respectively. The wild-type allele appeared in only one female (4%). There was an alteration from Mendelian inheritance according to the sex of the animals. Two-thirds of the population was female, so male offspring was underrepresented by 14% compared to the total number of animals. This difference might be due to the small sample size (28 pups in total). The female/male ratio showed the same pattern among all three mutated genotypes (70:30, 64:36, and 67:33 in $\Delta 128$, $\Delta 8$, and $\Delta 104$, respectively). The data are shown in Table 5. In the F2 generation, when a heterozygous male and female were bred, homozygous *NOX4* KO mutants of both sexes were born. We initialized the analyses of phenotype, such as litter size and preweaning lethality, and have not found any difference compared to wild-type litters. We have proof of homozygous animal survival and of the fertility of both sexes. More data with a higher sample size are needed to confirm or disprove the differences in sex ratio in *NOX4* knockout rabbits. The establishment of homozygous knockout population is in progress.

Table 5. Results of breeding of #5 founder male.

Rabbit Subline	$\Delta 128$	$\Delta 8$	$\Delta 104$	Wild-Type	Animals Born				
sex	♀	♂	♀	♂	♀	♂	♀	♂	
number of animals	7	3	9	5	2	1	1	0	28
ratio to total (%)	25%	11%	32%	18%	7%	3.50%	3.50%	0	
ratio of genotype to total (%)		36%		50%		10%		4%	
sex ratio within genotype (%)	70%	30%	64%	36%	67%	33%	100%	0%	
sex ratio (%)	♀	19	68%						
	♂	9	32%						

4. Discussion

The results of our study show the successful generation of several NADPH oxidase 4 knockout rabbit lines. The *NOX4* gene plays an important role in biological processes, and reactive oxygen species have a modulatory effect on the physiological functions of diverse mammal organs. *NOX4* knockout mouse models have recently been demonstrated to be useful models to study the regulation of insulin secretion [55]. Other research has shown the role of *NOX4* in liver fibrosis in connection with gut microbiota [56]. In addition, the protective effect of *NOX4* knockdown has also been demonstrated

in sepsis-induced lung injury in mice [57]. The broad spectrum of NOX4 function creates the need for better animal models to make the best mammalian system for the purposes of translational medicine.

The efficiency of CRISPR/Cas9 to induce site specific mutations in rabbits is a complex issue. Chromatin structure of the targeted genomic region affects the availability of the site to CRISPR/Cas9 complexes. An open chromatin structure predicts greater efficiency. The concentration of gRNA is also a crucial element. The encountered 16–18% efficiency of mutated blastocysts is within the normal range. However, the efficiency of targeting varies greatly between 10–100% according to scientific data [1].

Five founder animals were generated in total, of which three acquired identical 8 bp deletions. This phenomenon seems striking, but robust analysis of CRISPR-mediated genome editing in cell culture systems has shown that DNA editing varies considerably between sites, with some targets shown to have a highly preferred indel while others display a wide range of infrequent indels [58]. Presumably, the pattern is dependent on both DNA sequence and chromatin structure.

Interestingly, one of the *NOX4* KO founder males turned out to be a genetic mosaic animal with germline transmission of three distinct knockout alleles besides the wild-type allele to its offspring. The $\Delta 8$ subline of founder animal #5 carried a short 8 bp deletion directly upstream of the PAM site, which is a common type of modification induced by the CRISPR/Cas9 method according to our own observations and the literature [59]. The other two modified alleles carried longer deletions, a 128 bp deletion in the case of the $\Delta 128$ subline, and a more exciting deletion-insertion-rearrangement type of modification in the case of the $\Delta 104$ rabbit subline. Complex targeting events in genome-edited animals have previously been detected [60]. Both modifications— $\Delta 104$ and $\Delta 128$ —make the detection of the knockout allele a simple one-step procedure, with allele-specific PCR sparing us the burden of T7 assays in our future experiments.

We found a deviation of the male/female ratio from the expected Mendelian pattern of inheritance: 14% fewer males were born in the F1 litters of the #5 founder male. These data must be closely examined in our future studies and while evaluating F2-generation data.

Mosaic events during genome editing are generally unwanted events. There are known strategies to reduce the genetic mosaicism produced by CRISPR/Cas9 system [61]. Mosaic events can be found during rabbit genome editing using CRISPR/Cas9 methods after allele screening [2,8,62–66]. Our opinion is that mosaic events can be useful in animal models of human diseases. To profit from the fact that mosaic animals represent different edited alleles, we developed a new breeding strategy (Figure 6).

The mosaic animal is mated consecutively with its counterpart, resulting in litters whose newborns are closely related but represent different transgenic lines with different targeting events. We suppose that analyzing these lines would result in predictable and equal phenotypic differences, ensuring the observations are the outcome of genome editing but not off-target events. On the other hand, mosaic founders are mated with different genetic background partners, which will result in a population of newborns with a diverse genetic heritage. In this case, small differences during phenotyping are tolerated and can presumably be explained. Most of human diseases are multifactorial and multigenic. Even single inheritance disorders can show diverse appearance depending on genetic background. To create the best animal model of the analyzed disorder, it is necessary to keep genetic divergence within the model population. On the other hand, genetic diversity can cause uninterpretable deviations sometimes. This is one important reason why most studies use inbred mice as model animals. Inbred strains usually react in a predictable way. Our breeding strategy involved combining the advantages of inbred and diverse genetic populations. Although this strategy uses more animals and the phenotypic examination is more complex, the resulted biological answer closely resembles the progression of human diseases. Using our new mating system, genetically divergent and homogeneous genome-edited populations can be produced in parallel, which is beneficial in translational medicine studies.

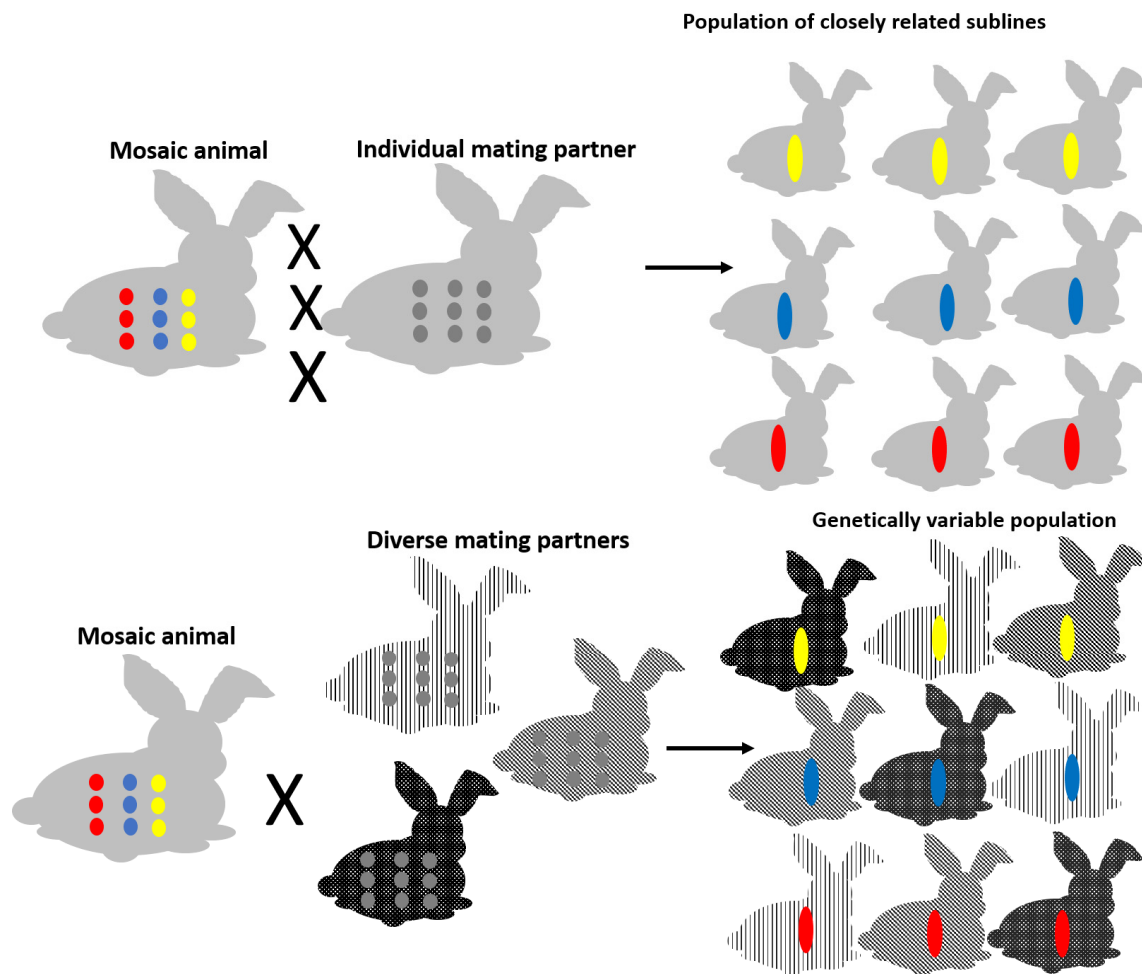


Figure 6. Optimal breeding strategy for generation of transgenic mosaic founder animals for use in translational medicine. Colored dots represent different mosaic alleles of a gene of interest, while colored rods represent inherited alleles in the F1 generation. The different gray background of rabbits highlights the variation in the genetic background.

Author Contributions: Conceptualization, M.G., Z.B. and L.H.; Data curation, M.G., L.H. and L.B.; Formal analysis, L.H. and L.B.; Funding acquisition, M.G. and Z.B.; Investigation, T.P., M.G., Z.B., L.H. and L.B.; Methodology, T.P., G.L.P., M.M., N.L., A.K. and L.B.; Resources, M.M. and N.L.; Validation, T.P., G.L.P. and G.S.; Visualization, L.B.; Writing—original draft, L.H. and L.B.; Writing—review & editing, M.G., N.L. and Z.B. All authors have read and agreed to the published version of the manuscript.

Funding: This research was funded by the Hungarian NVKP Grant No. NVKP_16-1-2016-0039 and by grant from the National Research Development and Innovation Office (K119955).

Conflicts of Interest: The authors declare no conflict of interest.

References

1. Yang, D.; Xu, J.; Zhu, T.; Fan, J.; Lai, L.; Zhang, J.; Chen, Y.E. Effective gene targeting in rabbits using RNA-guided Cas9 nucleases. *J. Mol. Cell Biol.* **2014**, *6*, 97–99. [[CrossRef](#)] [[PubMed](#)]
2. Guo, R.; Wan, Y.; Xu, D.; Cui, L.; Deng, M.; Zhang, G.; Jia, R.; Zhou, W.; Wang, Z.; Deng, K.; et al. Generation and evaluation of Myostatin knock-out rabbits and goats using CRISPR/Cas9 system. *Sci. Rep.* **2016**, *6*, 29855. [[CrossRef](#)] [[PubMed](#)]
3. Song, Y.; Xu, Y.; Deng, J.; Chen, M.; Lu, Y.; Wang, Y.; Yao, H.; Zhou, L.; Liu, Z.; Lai, L.; et al. CRISPR/Cas9-mediated mutation of tyrosinase (Tyr) 3' UTR induce graying in rabbit. *Sci. Rep.* **2017**, *7*, 1–8. [[CrossRef](#)] [[PubMed](#)]

4. Song, Y.; Sui, T.; Zhang, Y.; Wang, Y.; Chen, M.; Deng, J.; Chai, Z.; Lai, L.; Li, Z. Genetic deletion of a short fragment of glucokinase in rabbit by CRISPR/Cas9 leading to hyperglycemia and other typical features seen in MODY-2. *Cell. Mol. Life Sci.* **2020**, *77*, 3265–3277. [[CrossRef](#)]
5. Yuan, T.; Zhong, Y.; Wang, Y.; Zhang, T.; Lu, R.; Zhou, M.; Lu, Y.; Yan, K.; Chen, Y.; Hu, Z.; et al. Generation of hyperlipidemic rabbit models using multiple sgRNAs targeted CRISPR/Cas9 gene editing system. *Lipids Health Dis.* **2019**, *18*, 1–9. [[CrossRef](#)]
6. Sui, T.; Lau, Y.S.; Liu, D.; Liu, T.; Xu, L.; Gao, Y.; Lai, L.; Li, Z.; Han, R. A novel rabbit model of Duchenne muscular dystrophy generated by CRISPR/Cas9. *DMM Dis. Model. Mech.* **2018**, *11*, 1–9. [[CrossRef](#)]
7. Li, H.; Li, Z.; Xiao, N.; Su, X.; Zhao, S.; Zhang, Y.; Cui, K.; Liu, Q.; Shi, D. Site-specific integration of rotavirus VP6 gene in rabbit β -casein locus by CRISPR/Cas9 system. *Vitr. Cell. Dev. Biol.-Anim.* **2019**, *55*, 586–597. [[CrossRef](#)]
8. Yang, D.; Song, J.; Zhang, J.; Xu, J.; Zhu, T.; Wang, Z.; Lai, L.; Chen, Y.E. Identification and characterization of rabbit ROSA26 for gene knock-in and stable reporter gene expression. *Sci. Rep.* **2016**, *6*, 25161. [[CrossRef](#)]
9. Liu, H.; Sui, T.; Liu, D.; Liu, T.; Chen, M.; Deng, J.; Xu, Y.; Li, Z. Multiple homologous genes knockout (KO) by CRISPR/Cas9 system in rabbit. *Gene* **2018**, *647*, 261–267. [[CrossRef](#)]
10. Liu, Z.; Chen, M.; Chen, S.; Deng, J.; Song, Y.; Lai, L.; Li, Z. Highly efficient RNA-guided base editing in rabbit. *Nat. Commun.* **2018**, *9*, 1–10. [[CrossRef](#)]
11. Yang, D.; Zhang, J.; Xu, J.; Zhu, T.; Fan, Y.; Fan, J.; Chen, Y.E. Production of apolipoprotein C-III knockout rabbits using zinc finger nucleases. *J. Vis. Exp.* **2013**, *81*, 1–7. [[CrossRef](#)] [[PubMed](#)]
12. Lozano, W.M.; Arias-Mutis, O.J.; Calvo, C.J.; Chorro, F.J.; Zarzoso, M. Diet-induced rabbit models for the study of metabolic syndrome. *Animals* **2019**, *9*, 463. [[CrossRef](#)] [[PubMed](#)]
13. Fan, J.; Kitajima, S.; Watanabe, T.; Xu, J.; Zhang, J.; Liu, E.; Chen, Y.E. Rabbit models for the study of human atherosclerosis: From pathophysiological mechanisms to translational medicine. *Pharmacol. Ther.* **2015**, *146*, 104–119. [[CrossRef](#)] [[PubMed](#)]
14. Baumgartner, C.; Brandl, J.; Münch, G.; Ungerer, M. Rabbit models to study atherosclerosis and its complications—Transgenic vascular protein expression In Vivo. *Prog. Biophys. Mol. Biol.* **2016**, *121*, 131–141. [[CrossRef](#)] [[PubMed](#)]
15. Bószé, Z.; Major, P.; Baczkó, I.; Odening, K.E.; Bodrogi, L.; Hiripi, L.; Varró, A. The potential impact of new generation transgenic methods on creating rabbit models of cardiac diseases. *Prog. Biophys. Mol. Biol.* **2016**, *121*, 123–130. [[CrossRef](#)]
16. Koike, T.; Liang, J.; Wang, X.; Ichikawa, T.; Shiomi, M.; Liu, G.; Sun, H.; Kitajima, S.; Morimoto, M.; Watanabe, T.; et al. Overexpression of Lipoprotein Lipase in Transgenic Watanabe Heritable Hyperlipidemic Rabbits Improves Hyperlipidemia and Obesity. *J. Biol. Chem.* **2004**, *279*, 7521–7529. [[CrossRef](#)]
17. Jolivet, G.; Braud, S.; DaSilva, B.; Passet, B.; Harscoët, E.; Viglietta, C.; Gautier, T.; Lagrost, L.; Daniel-Carlier, N.; Houdebine, L.M.; et al. Induction of body weight loss through RNAi- knockdown of APOBEC1 gene expression in transgenic rabbits. *PLoS ONE* **2014**, *9*, e106655. [[CrossRef](#)]
18. Gonzalez-Bulnes, A.; Chavatte-Palmer, P. Contribution of Large Animals to Translational Research on Prenatal Programming of Obesity and Associated Diseases. *Curr. Pharm. Biotechnol.* **2017**, *18*, 541–551. [[CrossRef](#)]
19. Osteil, P.; Moulin, A.; Santamaria, C.; Joly, T.; Juneau, L.; Aubry, M.; Tapponnier, Y.; Archilla, C.; Schmaltz-Panneau, B.; Lecardonnel, J.; et al. A Panel of Embryonic Stem Cell Lines Reveals the Variety and Dynamic of Pluripotent States in Rabbits. *Stem. Cell Rep.* **2016**, *7*, 383–398. [[CrossRef](#)]
20. Tancos, Z.; Nemes, C.; Polgar, Z.; Gocza, E.; Daniel, N.; Stout, T.A.E.; Maraghechi, P.; Purity, M.K.; Osteil, P.; Tapponnier, Y.; et al. Generation of rabbit pluripotent stem cell lines. *Theriogenology* **2012**, *78*, 1774–1786. [[CrossRef](#)]
21. Quan, L.; Chen, Y.; Song, J.; Yan, Q.; Zhang, Q.; Lai, S.; Fan, N.; Xin, J.; Zou, Q.; Lai, L. Establishment of a rabbit Oct4 promoter-based EGFP reporter system. *PLoS ONE* **2014**, *9*, e109728. [[CrossRef](#)]
22. Zhang, S.; Xiang, S.; Yang, J.; Shi, J.; Guan, X.; Jiang, J.; Wei, Y.; Luo, C.; Shi, D.; Lu, F. Optimization of parthenogenetic activation of rabbit oocytes and development of rabbit embryo by somatic cell nuclear transfer. *Reprod. Domest. Anim.* **2019**, *54*, 258–269. [[CrossRef](#)]
23. Barman, A.; Deb, B.; Chakraborty, S. A glance at genome editing with CRISPR–Cas9 technology. *Curr. Genet.* **2020**, *66*, 447–462. [[CrossRef](#)] [[PubMed](#)]

24. Adli, M. The CRISPR tool kit for genome editing and beyond. *Nat. Commun.* **2018**, *9*, 1–13. [[CrossRef](#)] [[PubMed](#)]
25. Sakurai, T.; Watanabe, S.; Kamiyoshi, A.; Sato, M.; Shindo, T. A single blastocyst assay optimized for detecting CRISPR/Cas9 system-induced indel mutations in mice. *BMC Biotechnol.* **2014**, *14*, 1–11. [[CrossRef](#)] [[PubMed](#)]
26. Kleinstiver, B.P.; Pattanayak, V.; Prew, M.S.; Tsai, S.Q.; Nguyen, N.T.; Zheng, Z.; Keith Joung, J. High-fidelity CRISPR-Cas9 variants with undetectable genome-wide off-targets. *Nature* **2016**, *528*, 490–495. [[CrossRef](#)]
27. Anderson, K.R.; Haeussler, M.; Watanabe, C.; Janakiraman, V.; Lund, J.; Modrusan, Z.; Stinson, J.; Bei, Q.; Buechler, A.; Yu, C.; et al. CRISPR off-target analysis in genetically engineered rats and mice. *Nat. Methods* **2018**, *15*, 512–514. [[CrossRef](#)]
28. Mehravar, M.; Shirazi, A.; Nazari, M.; Banan, M. Mosaicism in CRISPR/Cas9-mediated genome editing. *Dev. Biol.* **2019**, *445*, 156–162. [[CrossRef](#)]
29. Yen, S.-T.; Zhang, M.; Deng, J.M.; Usman, S.J.; Smith, C.N.; Parker-Thornburg, J.; Swinton, P.G.; Martin, J.F.; Behringer, R.R. Somatic mosaicism and allele complexity induced by CRISPR/Cas9 RNA injections in mouse zygotes. *Dev. Biol.* **2014**, *393*, 3–9. [[CrossRef](#)]
30. Mizuno, S.; Thi, T.; Dinh, H.; Kato, K. Simple generation of albino C57BL/6J mice with G291T mutation in the tyrosinase gene by the CRISPR/Cas9 system. *Mamm. Genome* **2014**, *25*, 327–334. [[CrossRef](#)]
31. Sultana, F.; Hatori, M.; Shimozawa, N.; Ebisawa, T.; Sankai, T. Continuous observation of rabbit preimplantation embryos *in vitro* by using a culture device connected to a microscope. *J. Am. Assoc. Lab. Anim. Sci.* **2009**, *48*, 52–56. [[PubMed](#)]
32. Hiripi, L.; Negre, D.; Cosset, F.L.; Kvell, K.; Czömpöly, T.; Baranyi, M.; Gócza, E.; Hoffmann, O.; Bender, B.; Bosze, Z. Transgenic rabbit production with simian immunodeficiency virus-derived lentiviral vector. *Transgenic Res.* **2010**, *19*, 799–808. [[CrossRef](#)] [[PubMed](#)]
33. Atashi, F.; Modarressi, A.; Pepper, M.S. The role of reactive oxygen species in mesenchymal stem cell adipogenic and osteogenic differentiation: A review. *Stem Cells Dev.* **2015**, *24*, 1150–1163. [[CrossRef](#)] [[PubMed](#)]
34. Yao, M.I.N.; Gao, F.; Wang, X.; Shi, Y.; Liu, S.; Duan, H. Nox4 is involved in high glucose—induced apoptosis in renal tubular epithelial cells via Notch pathway. *Mol. Med. Rep.* **2017**, *15*, 4319–4325. [[CrossRef](#)]
35. Grandvaux, N.; Soucy-faulkner, A.; Fink, K. Innate host defense: Nox and Duox on phox’s tail. *Biochimie* **2007**, *89*, 1113–1122. [[CrossRef](#)]
36. Feng, C.; Zhang, Y.; Yang, M.; Lan, M.; Liu, H.; Huang, B.; Zhou, Y. Oxygen-Sensing Nox4 Generates Genotoxic ROS to Induce Premature Senescence of Nucleus Pulposus Cells through MAPK and NF- κ B Pathways. *Oxid. Med. Cell Longev.* **2017**, *2017*, 7426458. [[CrossRef](#)]
37. Liu, C.; Hua, N.; Fu, X.; Pan, Y.; Li, B.; Li, X. Metformin Regulates the Expression of SK2 and SK3 in the Atria of Rats with Type 2 Diabetes Mellitus Through the NOX4 / p38MAPK Signaling Pathway. *Cardiovasc. Pharmacol.* **2018**, *72*, 205–213. [[CrossRef](#)]
38. Song, S.; Xiao, X.; Guo, D.; Mo, L.; Bu, C.; Ye, W.; Den, Q.; Liu, S.; Yang, X. Phytomedicine Protective effects of Paeoni florin against AOPP-induced oxidative injury in HUVECs by blocking the ROS-HIF-1 α / VEGF pathway. *Phytomedicine* **2017**, *34*, 115–126. [[CrossRef](#)]
39. Yang, Q.; Wu, F.; Wang, J.; Gao, L.; Wei, B.; Zhou, L.; Wen, J.; Ma, T. Nox4 in Renal Diseases: An Update. *Free Radic. Biol. Med.* **2018**, *124*, 466–472. [[CrossRef](#)]
40. Radermacher, K.A.; Wingler, K.; Langhauser, F.; Altenho, S.; Kleikers, P.; Hermans, J.J.R.; Hrabe, M.; Kleinschnitz, C.; Schmidt, H.H.H.W. Neuroprotection After Stroke by Targeting NOX4 As a Source of Oxidative Stress. *Antioxid. Redox. Signal.* **2013**, *18*, 1418–1427. [[CrossRef](#)]
41. Meng, Y.; Li, T.; Zhou, G.-S.; Chen, Y.; Yu, C.-H.; Pang, M.-X.; Li, W.; Li, Y.; Zhang, W.-Y.; Li, X. The angiotensin-converting enzyme 2/angiotensin (1-7)/Mas axis protects against lung fibroblast migration and lung fibrosis by inhibiting the NOX4-derived ROS-mediated RhoA/Rho kinase pathway. *Antioxid. Redox Signal.* **2015**, *22*, 241–258. [[CrossRef](#)] [[PubMed](#)]
42. Nlandu Khodo, S.; Dizin, E.; Sossauer, G.; Szanto, I.; Martin, P.-Y.; Feraille, E.; Krause, K.H.; de Seigneux, S. NADPH-oxidase 4 protects against kidney fibrosis during chronic renal injury. *J. Am. Soc. Nephrol.* **2012**, *23*, 1967–1976. [[CrossRef](#)] [[PubMed](#)]
43. Lozhkin, A.; Vendrov, A.E.; Pan, H.; Wickline, S.A.; Nageswara, R.; Runge, M.S. NADPH oxidase 4 regulates vascular inflammation in aging and atherosclerosis. *J. Mol. Cell Cardiol.* **2017**, *102*, 10–21. [[CrossRef](#)] [[PubMed](#)]

44. Schürmann, C.; Rezende, F.; Kruse, C.; Yasar, Y.; Löwe, O.; Fork, C.; Van De Sluis, B.; Bremer, R.; Weissmann, N.; Shah, A.M.; et al. The NADPH oxidase Nox4 has anti-atherosclerotic functions. *Eur. Heart J.* **2015**, *36*, 3447–3456. [[CrossRef](#)]
45. Fan, J.; Chen, Y.; Yan, H.; Niimi, M.; Wang, Y.; Liang, J. Principles and Applications of Rabbit Models for Atherosclerosis Research. *J. Atheroscler. Thromb.* **2018**, *25*, 213–220. [[CrossRef](#)]
46. Faggion, C.M. Animal research as a basis for clinical trials. *Eur. J. Oral Sci.* **2015**, *123*, 61–64. [[CrossRef](#)]
47. Bailey, J.; Thew, M.; Balls, M. An Analysis of the Use of Animal Models in Predicting Human Toxicology and Drug Safety. *Altern. Lab. Anim.* **2014**, *42*, 181–199. [[CrossRef](#)]
48. Box, R.J.; Spielmann, H. Use of the dog as non-rodent test species in the safety testing schedule associated with the registration of crop and plant protection products (pesticides): Present status. *Arch. Toxicol.* **2005**, *79*, 615–626. [[CrossRef](#)]
49. Gilmore, K.M.; Greer, K.A. Why is the dog an ideal model for aging research? *Exp. Gerontol.* **2015**, *71*, 14–20. [[CrossRef](#)]
50. Burkhardt, A.M.; Zlotnik, A. Translating translational research: Mouse models of human disease. *Cell. Mol. Immunol.* **2013**, *10*, 373–374. [[CrossRef](#)]
51. Perlman, R.L. Mouse models of human disease an evolutionary perspective. *Evol. Med. Public Health* **2016**, *2016*, 170–176. [[CrossRef](#)] [[PubMed](#)]
52. Ivics, Z.; Hiripi, L.; Hoffmann, O.I.; Mátés, L.; Yau, T.Y.; Bashir, S.; Zidek, V.; Landa, V.; Geurts, A.; Pravenec, M.; et al. Germline transgenesis in rabbits by pronuclear microinjection of Sleeping Beauty transposons. *Nat. Protoc.* **2014**, *9*, 794–809. [[CrossRef](#)] [[PubMed](#)]
53. Sambrook, J.; Russell, D.W. *Molecular Cloning: A Laboratory Manual*, 4th ed.; Cold Spring Harbor Laboratory Press: Cold Spring Harbor, NY, USA, 2012; ISBN 978-1-936113-42-2.
54. Imanishi, M.; Negi, S.; Sugiura, Y. Non-FokI-based zinc finger nucleases. *Methods Mol. Biol.* **2010**, *649*, 337–349. [[CrossRef](#)] [[PubMed](#)]
55. Plecítá-hlavatá, L.; Jab, M.; Holendová, B.; Tauber, J.; Berková, Z.; Cahová, M.; Schröder, K.; Brandes, R.P.; Siemen, D.; Je, P. Glucose-Stimulated Insulin Secretion Fundamentally Requires H₂O₂ Signaling by NADPH Oxidase 4. *Diabetes* **2020**, *69*, 1341–1354. [[CrossRef](#)] [[PubMed](#)]
56. Wan, S.; Nie, Y.; Zhang, Y.; Huang, C.; Zhu, X. Gut Microbial Dysbiosis Is Associated with Profibrotic Factors in Liver Fibrosis Mice. *Front. Cell. Infect. Microbiol.* **2020**, *10*, 1–12. [[CrossRef](#)] [[PubMed](#)]
57. Jiang, J.; Huang, K.; Xu, S.; Garcia, J.G.N.; Wang, C.; Cai, H. Redox Biology Targeting NOX4 alleviates sepsis-induced acute lung injury via attenuation of redox-sensitive activation of CaMKII/ERK1/2/MLCK and endothelial cell barrier dysfunction. *Redox Biol.* **2020**, *36*, 101638. [[CrossRef](#)] [[PubMed](#)]
58. Chakrabarti, A.M.; Henser-brownhill, T.; Monserrat, J.; Poetsch, A.R.; Luscombe, N.M.; Scaffidi, P. Target-Specific Precision of CRISPR-Mediated Genome Editing. *Mol. Cell* **2019**, *73*, 699–713. [[CrossRef](#)]
59. Labun, K.; Guo, X.; Chavez, A.; Church, G.; Gagnon, J.A.; Valen, E. Accurate analysis of genuine CRISPR editing events with ampliCan. *Genome Res.* **2019**, *29*, 843–847. [[CrossRef](#)]
60. Shin, H.Y.; Wang, C.; Lee, H.K.; Yoo, K.H.; Zeng, X.; Kuhns, T.; Yang, C.M.; Mohr, T.; Liu, C.; Hennighausen, L. CRISPR/Cas9 targeting events cause complex deletions and insertions at 17 sites in the mouse genome. *Nat. Commun.* **2017**, *8*, 15464. [[CrossRef](#)]
61. Lamas-Toranzo, I.; Galiano-Cogolludo, B.; Cornudella-Ardiaca, F.; Cobos-Figueroa, J.; Ousinde, O.; Bermejo-Álvarez, P. Strategies to reduce genetic mosaicism following CRISPR-mediated genome edition in bovine embryos. *Sci. Rep.* **2019**, *9*, 14900. [[CrossRef](#)]
62. Yan, Q.; Zhang, Q.; Yang, H.; Zou, Q.; Tang, C.; Fan, N. Generation of multi-gene knockout rabbits using the Cas9 / gRNA system. *Cell Regen.* **2014**, *3*, 1–11. [[CrossRef](#)] [[PubMed](#)]
63. Honda, A.; Hirose, M.; Sankai, T.; Yasmin, L. Single-step generation of rabbits carrying a targeted allele of the tyrosinase gene using CRISPR / Cas9. *Exp. Anim.* **2015**, *64*, 31–37. [[CrossRef](#)] [[PubMed](#)]
64. Lv, Q.; Yuan, L.; Deng, J.; Chen, M.; Wang, Y.; Zeng, J.; Li, Z.; Lai, L. Efficient Generation of Myostatin Gene Mutated Rabbit by CRISPR/Cas9. *Sci. Rep.* **2016**, *6*, 25029. [[CrossRef](#)] [[PubMed](#)]
65. Song, Y.; Yuan, L.; Wang, Y.; Chen, M.; Deng, J.; Lv, Q.; Sui, T.; Li, Z.; Lai, L. Efficient dual sgRNA-directed large gene deletion in rabbit with CRISPR/Cas9 system. *Cell. Mol. Life Sci.* **2016**, *73*, 2959–2968. [[CrossRef](#)] [[PubMed](#)]

66. Yuan, L.; Sui, T.; Chen, M.; Deng, J.; Huang, Y.; Zeng, J.; Lv, Q.; Song, Y.; Li, Z.; Lai, L. OPEN CRISPR / Cas9-mediated GJA8 knockout in rabbits recapitulates human congenital cataracts. *Sci. Rep.* **2016**, *6*, 22024. [[CrossRef](#)]

Publisher's Note: MDPI stays neutral with regard to jurisdictional claims in published maps and institutional affiliations.



© 2020 by the authors. Licensee MDPI, Basel, Switzerland. This article is an open access article distributed under the terms and conditions of the Creative Commons Attribution (CC BY) license (<http://creativecommons.org/licenses/by/4.0/>).